ACS APPLIED MATERIALS & INTERFACES

Research Article

www.acsami.org

Highly Enhanced Fluorescence of CdSeTe Quantum Dots Coated with Polyanilines via In-Situ Polymerization and Cell Imaging Application

Jingjing Xue, Xinyi Chen, Shanglin Liu, Fenfen Zheng, Li He, Lingling Li,* and Jun-Jie Zhu*

State Key Laboratory of Analytical Chemistry for Life Science, Collaborative Innovation of Chemistry for Life Science, School of Chemistry and Chemical Engineering, Nanjing University, Nanjing 210093, China

ABSTRACT: The polyaniline (PAN)-coated CdSeTe quantum dots (QDs) were prepared by in situ polymerization of aniline on the surface of CdSeTe QDs. The PAN-coated CdSeTe QDs has a tremendously enhanced fluorescence (~40 times) and improved biocompatibility compared to the uncoated CdSeTe QDs. The fluorescence intensity of the PAN-coated CdSeTe QDs can be adjusted by controlling the construction parameters of the PAN shell. The kinetics of the in situ controllable polymerization process was studied by varying the temperature, and the apparent activation energy of polymerization was estimated. With the same method, a series of the PAN derivatives were also tested to coat the CdSeTe QDs in this study. All the QDs showed a significant enhancement of the fluorescence intensity and better biocompatibility. The significantly enhanced fluorescence can provide highly amplified signal for luminescence-based cell imaging.

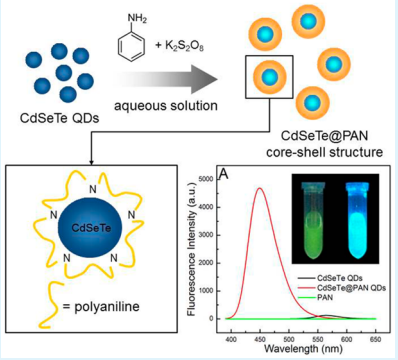

KEYWORDS: *quantum dots, polyanilines, enhanced fluorescence, in situ polymerization, cell imaging*

1. INTRODUCTION

Fluorescent semiconductor quantum dots have attracted great interest over the past years in various fields, for example, solar cells,[1−4] imaging,[5−8] light-emitting devices,[9−12] and biosensors,[13−16] since of their unique optical properties. However, the nanometric crystal size brings in a very high surface-to-volume ratio and thus high surface deficiency, which can adversely affect the optical performance of QDs. To reduce the surface deficiency of QDs, many methods have been developed to modify the surface structure of QDs. A significant strategy to improve QDs surface passivation is to decorate them with a shell of a second semiconductor.[17−19] It has been reported that the fluorescence quantum yield of QDs can be improved by the modification of a shell with a large band gap semiconductor.[20] Inorganic semiconductors, such as CdS, ZnS, and SiO_2 are now commonly used as appropriate shell materials to improve the optical properties.[21−26]

With regard to biological applications of semiconductor QDs, besides their eligible optical properties, biocompatibility is another key requirement. Compared with an inorganic shell, a polymeric one typically shows a better compatibility and could be a promising candidate for the shell material. Up to now, some methods of decorating QDs with hydrophilic polymer have been developed. Polyethylene glycol (PEG), polyethylene glycol-phosphatidyl ethanolamine copolymer (PEG−PE) and poly(methyl methacrylate) (PMMA) have been decorated onto QDs to improve their stability and biocompatibility,[27−32] and polyamide amine (PAMAM) has been grafted onto QDs to functionalize the initial QDs.[33−37] The fluorescence intensity and the quantum yields of the QDs prepared by some of the methods have been improved to a certain degree (~2 times),[36,37] but in most cases the fluorescence intensity of the QDs coated with such polymers has not been improved or even decreased, or the largely increased particle size resulted in some restrictions for their applications. Conducting polymers, such as polyaniline (PAN), polypyrrole (PPY) and polythiophene (PTH) have aroused great interest because of their attractive properties, for example, conductivity, mechanical flexibility, and biocompatibility.[38−41] The band gap of conducting polymers can be adjusted by controlling their degree of polymerization, rendering them the properties of a semiconductor. Thus, they are expected to be a promising shell material to produce QDs with stronger and controllable fluorescence as well as better biocompatibility. In our previous studies, water-soluble CdSeTe, CdSeTe/ZnS and CdSeTe/CdS/ZnS QDs have been prepared and successfully applied to biosensing.[42−44] Herein, PAN-coated CdSeTe QDs were obtained via an in situ polymerization method on particle surface. The PAN shell brought about a significant enhancement of the fluorescence intensity (~40 times) as well as improved biocompatibility. Several PAN derivations, that is, poly(*o*-methylaniline) (PMAN), poly(*m*-aminobenzoic acid) (PABA), and poly(*o*-chloroaniline) (PCAN), were also tested with this method. A tunable fluorescence can be achieved by varying either a polymer type or a degree of polymerization. The enhanced fluorescence can provide highly amplified signal for lumines-

Received: May 31, 2015
Accepted: August 13, 2015
Published: August 13, 2015

DOI: 10.1021/acsami.5b04766
ACS Appl. Mater. Interfaces 2015, 7, 19126−19133

cence-based cell imaging and is anticipated to be beneficial to other possible bioapplications.

2. EXPERIMENTAL SECTION

2.1. Materials. Aniline, *m*-aminobenzoic, toluidine, and *o*-chloroaniline were purchased from Nanjing Chemical Reagents Factory (Nanjing, China) and were purified by reduced pressure distillation. 3-(4,5-Dimethylthiazol-2-yl)-2,5-diphenyltetrazolium bromide (MTT) was purchased from Sigma (St.Louis, MO, USA). Secondary deionized water (18.2 MΩ·cm at 25 °C) prepared by a Milli-Q (MQ) water system was used throughout all experiments. All other reagents were of analytical grade and used as received.

2.2. Synthesis of CdSeTe QDs. The CdSeTe QDs were prepared according to our previous work.[42] $CdCl_2$ (0.625 mmol) and 3-mercaptopropionic acid (1.5 mmol) were dissolved in 500 mL of water, and pH was adjusted to 12.2 with 1 M of NaOH. The precursor solution was then loaded into a three-necked flask and stirred at 15 ± 2 °C in oxygen-free atmosphere under nitrogen for about 30 min. At this temperature, the mixed solution composed of 1.0 mL of fresh NaHTe aqueous solution and 0.5 mL of fresh NaHSe aqueous solution which were respectively prepared from $NaBH_4$ and Te powder (0.125 mmol) or Se powder (0.125 mmol) was injected into the reaction system under vigorous stirring. The solution was then stirred in oxygen-free atmosphere under nitrogen for 1 h to get CdSeTe nanoclusters which were then stored under 4 °C for 24 h. After purified by absolute ethanol and concentrated 10 times, the solution was then refluxed under 240 W in the microwave oven.

2.3. Synthesis of CdSeTe QDs Coated with PAN and Its Derivatives (CdSeTe@PANs QDs). The pH of CdSeTe QDs solution (500 μL) was adjusted to 6−7 with an appropriate amount of 0.1 M of HCl. 0.6875 μL of aniline (AN) was then added into the solution and fully mixed 2.7 mg of $K_2S_2O_8$ was then added into the mixture to initiate the reaction. The growth of polyaniline shell on the surface of CdSeTe QDs lasted for about 5 h at 25 ± 2 °C to obtain highly fluorescent CdSeTe@PAN QDs. The Schematic representation of the preparation of CdSeTe@PAN QDs is shown in Figure 1.

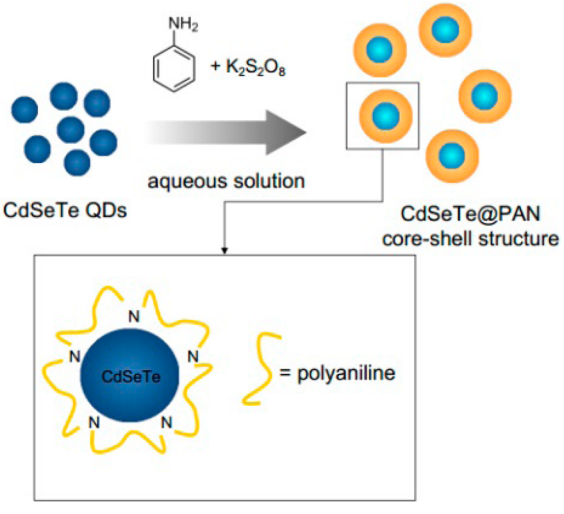

Figure 1. Schematic representation of the preparation of CdSeTe@PAN QDs.

The similar method has been used to prepare the PAN derivatives-capped CdSeTe QDs except that 0.5156 mg of *m*-aminobenzoic acid (ABA) monomer was used to obtain CdSeTe@PABA QDs, 0.7812 μL of *o*-methylaniline (MAN) and 0.1985 μL of *o*-chloroaniline (CAN) were used respectively for each type of QDs.

2.4. Sample Characterizations. An F-7000 spectrophotometer (Hitachi, Japan) set with an excitation slit width of 2.5 nm and an emission slit width of 2.5 nm was used to excite the samples (at 360 nm) to record their fluorescence spectra. Ultraviolet−visible (UV−vis) absorption spectra were obtained using a UV-3600 spectrophotometer (Shimadzu). Fluorescence quantum yield (QY) was determined using a previously published procedure by using rhodamine B as a reference standard. Fourier transform infrared (FTIR) spectra were taken on a Nicolet 6700 spectrophotometer (Nicolet, USA) using KBr pressed disks. High-resolution transmission electron microscopy (HRTEM) images were taken using a JEOL 2010 electron microscope operated at 200 kV. The HRTEM samples were prepared by drop casting one drop of a dilute solution of QDs on a carbon-coated copper grid. The grid was dried by evaporating the solvent in air. Zeta potential was measured on a nano Z zeta potential analyzer (Malvern Instruments, USA).

2.5. Quantum Yield (QY) calculations. The quantum yields of CdSeTe and CdSeTe@PANs QDs were obtained by comparing the integrated FL intensities and the absorbance values (at 360 nm) of the QDs with the references, rhodamine B (Φ = 0.31) and the as-prepared QDs were dissolved in water (n = 1.33). UV−vis absorption spectrometer was used to determine the absorbance values of the samples at a 360 nm excitation wavelength. The spectrophotometer set with an excitation slit width of 2.5 nm and an emission slit width of 2.5 nm was used to excite the samples 360 nm to record their FL spectra. The QY was calculated using the equation below[45]

$$\Phi_x = \Phi_r \times \frac{I_x}{I_r} \times \frac{A_x}{A_r} \times \frac{n_x^2}{n_r^2}$$

where Φ is the QY, I is the integrated fluorescence intensity, A is the absorbance, and n is the refractive index of the solvent; r denotes the standard and x denotes the sample.

2.6. Kinetic Study. The change of fluorescence intensity of QDs during the in situ capping process was monitored every 2 min. The monitoring experiments of the formation of CdSeTe@PAN, CdSeTe@PMAN, CdSeTe@PABA and CdSeTe@PCAN QDs were carried out at different temperatures (288.2, 293.2, 298.2, 303.2, 308.2, and 313.2 K). Subsequently, the initial reaction rate at different temperatures was measured and the activation energy of each polymerization could be determined using the Arrhenius equation.

2.7. Cellular Toxicity Test. The in vitro cytotoxicity of CdSeTe QDs and as-prepared CdSeTe@PANs QDs was evaluated by the MTT cell viability assay on human cervical carcinoma cells (HeLa cells). The MTT assay was carried out according to previously reported literature.[41] Briefly, HeLa cells were seeded in 96-well plates at 1 × 10^4 cells/well in Dulbecco's Modified Eagle's Medium (DMEM) with 10% fetal bovine serum and 100 μg/mL of penicillin/streptomycin and incubated at 37 °C in a humidified atmosphere with 5% CO_2. After incubating the cells for 24 h, the medium was replaced with 100 μL of fresh medium containing CdSeTe QDs or CdSeTe@PANs QDs with a concentration from 0 μg/mL to 100 μg/mL. After 24 h, the medium was removed and fresh medium (100 μL) containing MTT (10 μL, 5 mg/mL) was added into each well. After incubating the cells for 4 h, the absorbance of the solution was measured to assess the relative viability of the cells using a ThermoFisher Scientific Varioskan Flash multifunctional microplate reader. Optical density (OD) was read at a wavelength of 490 nm. The cell viability was estimated according to the following equation.

$$\text{cell viability (\%)} = \frac{\text{OD}_{\text{Treated}}}{\text{OD}_{\text{Control}}} \times 100\%$$

where $\text{OD}_{\text{Control}}$ is the optical density in the absence of QDs and $\text{OD}_{\text{Treated}}$ is the optical density in the presence of QDs.

2.8. Cell Imaging. HeLa cells were cultured in phosphate buffered saline (PBS) medium in a humidified atmosphere with 5% CO_2 inside an incubator at 37 °C (standard condition). For the celling imaging assay, the cells were washed with PBS and then incubated with 250 μL of a CdSeTe QDs solution (0.5 μM) and 250 μL of a CdSeTe@PABA QDs solution (0.5 μM) respectively for 2 h. After incubation, the cells were washed with PBS again and the labeling was observed under the confocal microscope (TCS SP5 Leica, Germany). CdSeTe QDs were excited with 360 nm laser and the signal was collected from 500 to 560

DOI: 10.1021/acsami.5b04766
ACS Appl. Mater. Interfaces 2015, 7, 19126−19133

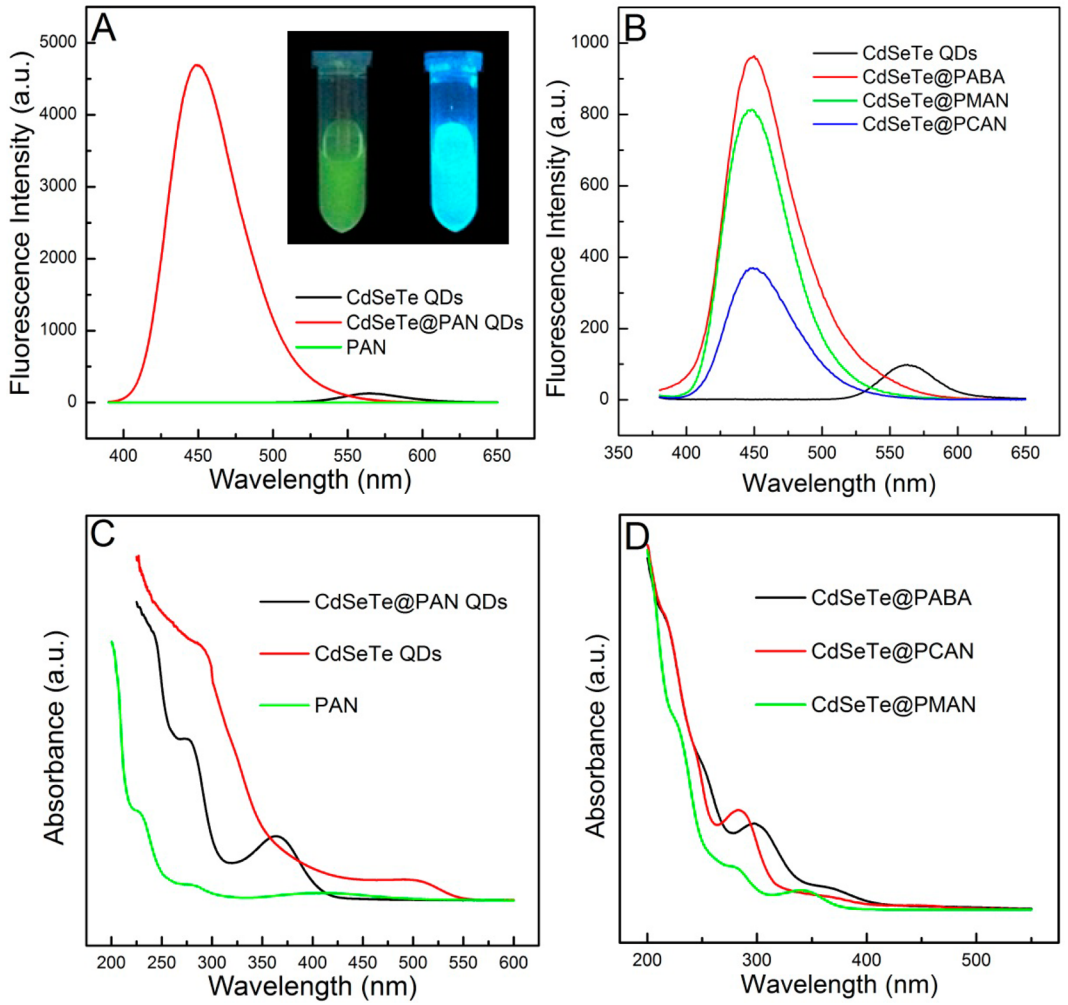

Figure 2. (A) Fluorescence spectra of CdSeTe QDs, CdSeTe@PAN QDs and PAN. Inset: Camera image of CdSeTe QDs (left) and CdSeTe@PAN QDs (right) in the exposure of ultraviolet light. (B) Fluorescence spectra of CdSeTe QDs, CdSeTe@PABA QDs, CdSeTe@PMAN QDs, and CdSeTe@PCAN QDs. (C) UV−vis absorbance spectra of CdSeTe QDs, CdSeTe@PAN QDs and PAN. (D) UV−vis absorbance spectra of CdSeTe QDs coated with PAN derivatives.

nm. CdSeTe@PABA QDs were excited with 360 nm laser and the signal was collected from 380 to 440 nm.

3. RESULTS AND DISCUSSION

3.1. Significant Enhancement of Fluorescence. The fluorescence and UV−vis spectra of CdSeTe QDs coated and uncoated with PANs are shown in Figure 2. Compared to the bare CdSeTe QDs, the fluorescence of QDs was dramatically improved via an in situ capping of either PAN or its derivatives on the surface of CdSeTe QDs (Figure 2A, B). During the growth of PANs shell, the fluorescence intensity of the bare CdSeTe QDs (560 nm) gradually decreased. Meanwhile, a new peak attributed to CdSeTe@PANs QDs appeared at around 450 nm and the intensity of this peak gradually increased. However, when the same amount of CdSeTe QDs was just mixed up with as-prepared PANs under the same condition, no enhanced fluorescence could be observed, indicating the existence of the in situ capping process. Via this in situ polymerization method, the ultimate fluorescence intensity of CdSeTe@PAN QDs is up to about 40 times stronger than the bare CdSeTe QDs (Figure 2A). For CdSeTe@PABA, CdSeTe@PMAN, and CdSeTe@PCAN QDs, the fluorescence intensity increased about 10, 8, and 4 times, respectively (Figure 2B). All QDs were excited at 360 nm as indicated by the UV−vis absorbance spectra (Figure 2C, D). As control experiments, pure PAN was prepared under the same conditions without CdSeTe QDs. The fluorescence and the UV−vis absorbance spectra of pure PAN is shown in Figure 2A and Figure 2C respectively. Figure 2A indicates that the pure PAN showed no fluorescence when excited at the same wavelength as QDs (360 nm). The UV−vis absorbance spectrum of pure PAN (Figure 2C) shows that there is no absorption peak at 360 nm, therefore pure PAN is non-fluorescent under such condition. The PAN derivatives also showed no fluorescence under the same condition without CdSeTe QDs, indicating that the fluorescence emission at 450 nm is attributed to QDs rather than PANs.

The great enhancement of fluorescence intensity is attributed to the surface passivation of CdSeTe QDs with PANs shell. When the QDs are unpassivated, the existence of surface states cause nonradioactive transition, which can reduce the radiative quantum yield.[46] However, when coated with a semiconductor with a wide band gap, the charge carriers are confined within the core region and separated from the surface owing to the enough offset of band gap energies between core and shell region, generating the significantly enhanced fluorescence.

DOI: 10.1021/acsami.5b04766
ACS Appl. Mater. Interfaces 2015, 7, 19126−19133

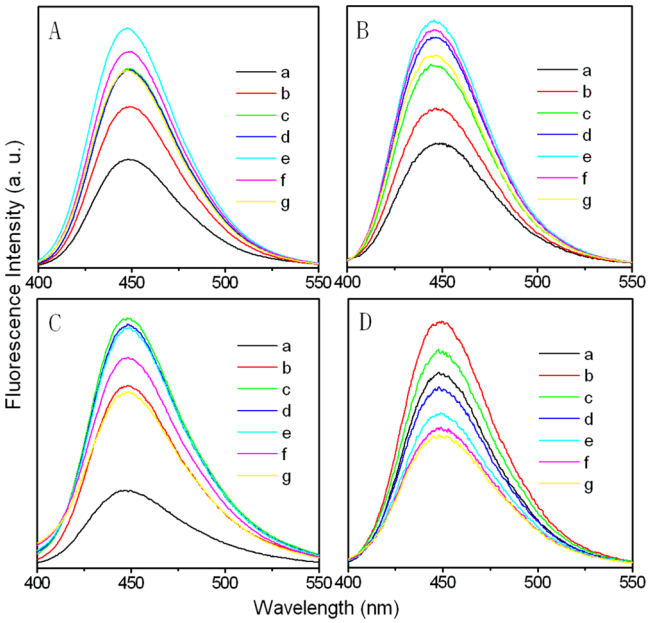

Figure 3. Fluorescence spectra of (A) CdSeTe@PAN QDs (B) CdSeTe@PMAN QDs (C) CdSeTe@PABA QDs (D) CdSeTe@PCAN QDs prepared via different molar ratio of monomer to CdSeTe QDs (r_m). (a) r_m = 1250; (b) r_m = 2500; (c) r_m = 5000; (d) r_m = 7500; (e) r_m = 10000; (f) r_m = 15000; (g) r_m = 20000.

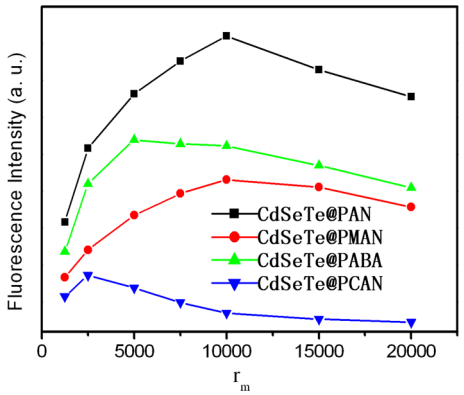

Figure 4. Relationship between the peak of fluorescence of CdSeTe@PANs QDs and r_m according to the data in Figure 3.

Table 1. Calculations of CdSeTe and PAN Derivative-Capped QDs

sample	integrated fluorescence intensity (I)	absorbance at 360 nm (A)	refractive index of the solvent (n)	quantum yield (Φ)
rhodamine B	55828	0.054	1.33	0.31
CdSeTe	12135	0.048	1.33	0.076
CdSeTe@PAN	102731	0.040	1.33	0.77
CdSeTe@PABA	84391	0.035	1.33	0.72
CdSeTe@PCAN	61318	0.041	1.33	0.45
CdSeTe@PMAN	48208	0.036	1.33	0.40

Once passivated by the conducting polymer shell, the surface defects are modified and generate intrinsic states of QDs. Since the band gap of defect states is smaller than that of intrinsic states of QDs,[47,48] the band edge emission of PANs-capped QDs shifted to a higher energy after the surface traps were passivated by PANs shell, resulting in the greatly increased fluorescence with a blue shift from 560 nm to about 450 nm.

The amount of monomers (AN, ABA, MAN, and CAN) plays an important role in the in situ coating process. When the amount of monomers was too small, the surface passivation of CdSeTe QDs could not be effectively improved while excessive monomers resulted in bulk polymers to quench the fluorescence. Several studies have been published regarding the preparation of CdSe/PAN or CdS/PAN nanocomposites. However, the fluorescence of QDs has not been effectively enhanced due to the excessive amount of PAN.[49,50] In this work, an appropriate molar ratio of the monomers to CdSeTe QDs ranging from 1250 to 20000 was chosen to obtain CdSeTe@PANs QDs with enhanced fluorescence.

Figure 3 shows the effect of the molar ratio of monomers to CdSeTe QDs (r_m) on the fluorescence intensity of the obtained CdSeTe@PANs QDs with a fixed amount of either CdSeTe QDs or the initiator $K_2S_2O_8$. It can be observed that the fluorescence intensity increased at first and then gradually decreased with the increase of r_m. Figure 4 shows the relationship between the peak of fluorescence and r_m according to the data in Figure 3. The results in Figure 4 indicate that there was an optimal concentration for each monomer to achieve maximal fluorescence intensity. With a monomer concentration below this optimal value, the surface coverage and the passivation of the CdSeTe core by the polymer improved as the degree of polymerization increased, so as the fluorescence intensity was increasing. Once the monomer concentration got higher than this optimal value, the polymer chains on the surface of CdSeTe grew further and the band gap of the conducting polymer would decrease. So the shell could not effectively confine the charge carriers within the core region, which could adversely affect the optical properties of QDs. Therefore, by changing the amount of the monomer and thus the degree of the polymerization, the fluorescence of QDs can be adjusted.

The quantum yields of the obtained CdSeTe@PANs QDs with the maximum fluorescence intensity using rhodamine B as a reference is 0.77, 0.72, 0.45, and 0.40, respectively, while the quantum yield of CdSeTe QDs is only 0.076 (Table 1). This considerable improvement in optical properties indicates that this kind of conducting polymers can be expected as a series of promising shell materials.

3.2. Characterizations. High resolution transmission electron microscopy (HRTEM) was used to characterize the as-prepared QDs. Taking CdSeTe@PAN QDs as an example, Figure 5 shows that CdSeTe QDs were confirmed to be nanoscale-sized with mean diameter of 2.5 nm while the corresponding CdSeTe@PAN QDs showed increased average size of 5 nm.

FTIR spectra were used to further verify the coating of PAN on the surface of CdSeTe QDs. Figure 6 shows FTIR spectra of CdSeTe QDs, PAN and CdSeTe@PAN QDs, respectively. The spectra of pure PAN show characteristic peaks at 1188 and 1363 cm^{-1} that can be attributed to the vibration of C−N bond in aromatic aniline and the peak at 1540 cm^{-1} corresponded to the characteristic vibration of the N−B−N structure (B represents the benzoid unit).[51] Both the spectra of CdSeTe and CdSeTe@PAN QDs show the characteristic peaks of CdSeTe QDs at 1307 and 1275 cm^{-1}. In the spectra of CdSeTe@PAN QDs, the characteristic peak of PAN corresponding to the vibration of C−N bond shifts from

DOI: 10.1021/acsami.5b04766
ACS Appl. Mater. Interfaces 2015, 7, 19126−19133

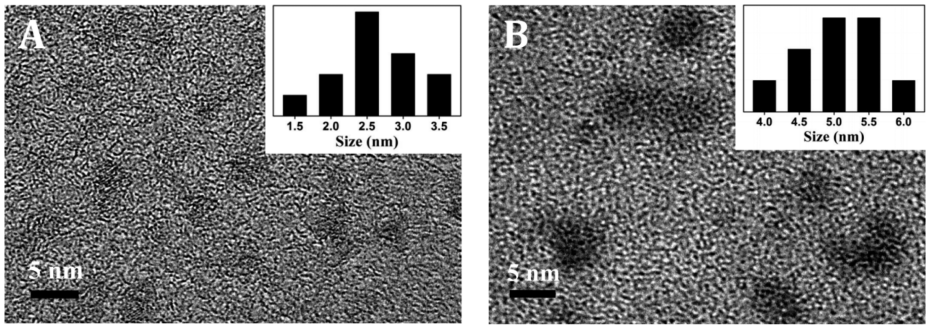

Figure 5. HRTEM images of (A) CdSeTe QDs and (B) CdSeTe@PAN QDs.

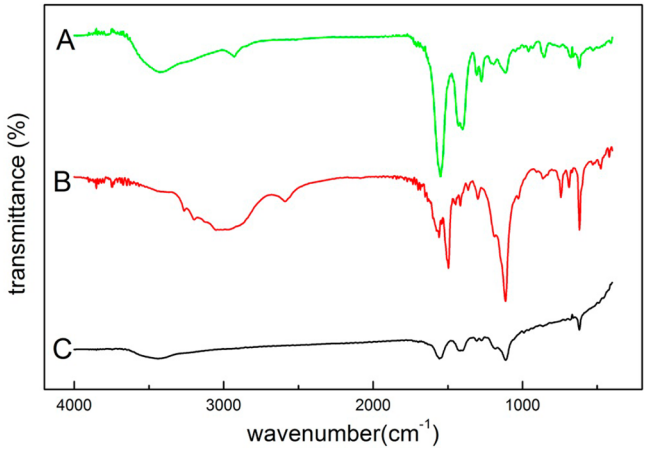

Figure 6. FTIR spectra of (A) CdSeTe QDs, (B) PAN, (C) CdSeTe@PAN QDs.

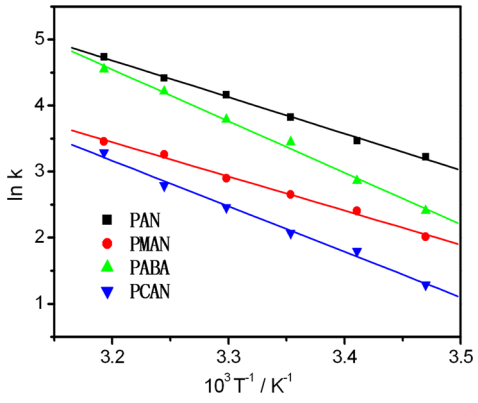

Figure 8. Relationship between ln k and $1/T$ according to the data in Figure 7 for in situ capping of PAN, PMAN, PABA, and PCAN on the surface of CdSeTe QDs.

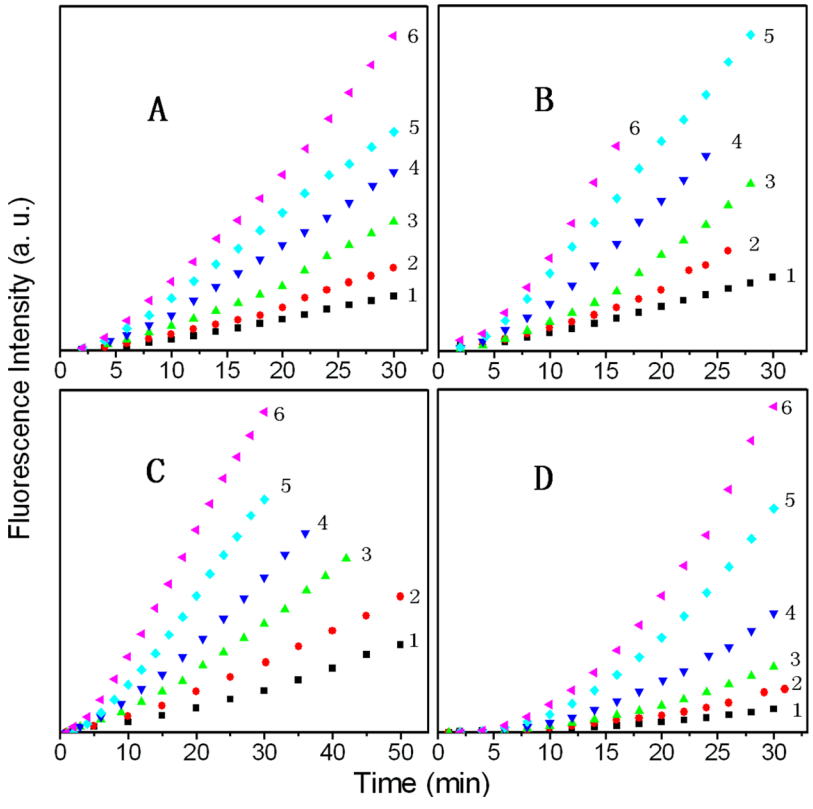

Figure 7. Relationship between fluorescence intensity and reaction time at various temperatures (1, 288.2 K; 2, 293.2 K; 3, 298.3 K; 4, 303.2 K; 5, 308.2 K; 6, 313.2 K): (A) CdSeTe@PAN QDs, (B) CdSeTe@PMAN QDs, (C) CdSeTe@PABA QDs, and (D) CdSeTe@PCAN QDs.

DOI: 10.1021/acsami.5b04766
ACS Appl. Mater. Interfaces 2015, 7, 19126−19133

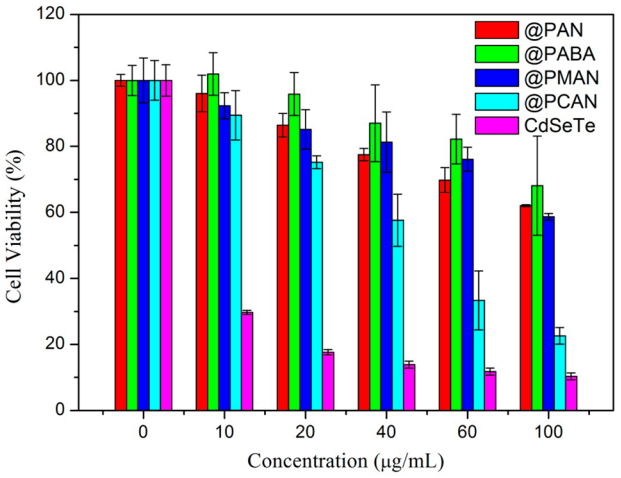

Figure 9. Growth inhibition assay (MTT) showing effects of either CdSeTe QDs or CdSeTe@PANs QDs on the viability of HeLa cells.

1188 to 1192 cm^{-1} and the peak of the vibration of N−B−N structure shifts from 1540 to 1548 cm^{-1}, indicating the electrostatic interactions between the CdSeTe core and the PAN shell through their carboxyl and amine groups. In addition, the zeta potential of the CdSeTe and CdSeTe@PAN QDs aqueous solution were measured to be −29.9 and −53.1 mV respectively, indicating that CdSeTe@ PAN QDs were more negatively charged. The increased surface charge could improve the colloidal stability of the nanoparticles because of an electrostatic repulsion.

3.3. Kinetics of the in Situ Capping Process. To study the kinetics of the in situ coating process, activation energies of the in situ polymerization of AN, ABA, MAN, and CAN on the surface of CdSeTe QDs were determined by monitoring the fluorescence intensity of QDs during the reactions at different temperatures. As shown in Figure 7, during the growth of PANs shell, a peak at around 450 nm of CdSeTe@PANs QDs occurred and the intensity gradually increased. Since the fluorescence intensity is proportional to the concentration in a certain range, we can use the ratio of fluorescence intensity to reaction time to represent the reaction rate. We calculated the slope of the curve as the average reaction rate (k). Figure 8 shows the relationship between ln k and $1/T$, where T is the reaction temperature in kelvin. The linear regression equations are $\ln k = 22.400 - 5.537/T$ (CdSeTe@PAN), $\ln k = 19.986 - 5.170/T$ (CdSeTe@PMAN), $\ln k = 29.560 - 7.817/T$ (CdSeTe@PABA), and $\ln k = 25.213 - 6.890/T$ (CdSeTe@PCAN), respectively. The activation energies were calculated by Arrhenius equation[52]

$$k = Ae^{-E_a/RT}$$

where A is the pre-exponential factor, E_a is the activation energy of the reactions, and R is the molar gas constant. The activation energy of the in situ polymerization of AN on CdSeTe QDs was measured to be 46.0 ± 1.2 kJ/mol, while those of MAN, ABA, and CAN are 43.0 ± 1.6, 65.0 ± 2.2, and 57.3 ± 2.5 kJ/mol, respectively. The introduction of electron-withdrawing group (−COOH and −Cl) reduces the density of electron moiety on the benzene rings, which results in the decrease in the rate of chain growth and the increase of activation energy.[53] The introduction of weak electron-donating group ($-CH_3$), on the contrary, increases the density of electron moiety and results in the slight decrease of activation energy. The calculated values of the activation energies are in the same order of magnitude of the activation energies of the polymerization of aniline reported in the literature.[54,55] The data trend of the activation energies of in situ polymerizations of aniline and its derivatives on the surface of CdSeTe QDs is in accord with the kinetic regularity of polymerizations of pure aniline and the corresponding derivatives. Such results of the kinetic study suggest the in situ growth of PANs on the surface of CdSeTe QDs and indicate the tunability and controllability of this capping process.

3.4. Cytotoxicity and Bioimaging. The in vitro cytotoxicity of CdSeTe@PANs QDs in comparison with the bare CdSeTe QDs was evaluated using HeLa cells with an MTT viability assay (Figure 9). Results suggest that CdSeTe@PANs QDs have lower toxicity to the HeLa cells than CdSeTe QDs did because of great biocompatibility of shell material. Among the as-prepared CdSeTe@PANs QDs, CdSeTe@PABA QDs showed the lowest cytotoxicity, which could be attributed to the introduction of a hydrophilic group to the PAN shell that can further improve the biocompatible of QDs. CdSeTe@PCAN QDs showed a relatively higher cytotoxicity compared to other CdSeTe@PANs QDs because PCAN contains organic chlorine resulting in its slight toxicity. PAN and PMAN have similar properties so the MTT results of the two were similar. The greatly enhanced QYs and excellent biocompatibility make the as-prepared conducting polymer-coated QDs suitable for biomedical applications. Thus, we applied CdSeTe@PABA QDs with the lowest toxicity to cell imaging experiments to further evaluate their bioimaging applications. Figure 10 shows the images of HeLa cells treated with CdSeTe and CdSeTe@PABA QDs for 2 h, respectively. Obviously, the HeLa cells

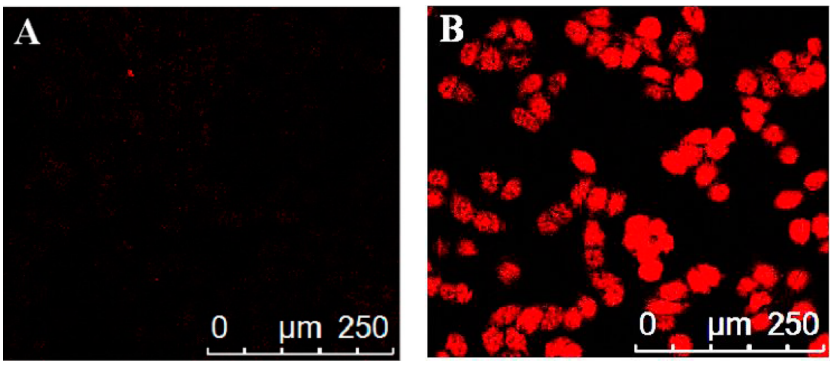

Figure 10. Fluorescent images of (A) HeLa cells cultured with CdSeTe QDs and (B) HeLa cells cultured with CdSeTe@PABA QDs.

DOI: 10.1021/acsami.5b04766
ACS Appl. Mater. Interfaces 2015, 7, 19126−19133

treated with CdSeTe@PABA QDs displayed highly amplified signal compared to those cultured with the bare CdSeTe QDs.

4. CONCLUSIONS

In this study, we prepared CdSeTe QDs coated with a series of conducting polymers (i.e., PANs) via an in situ polymerization method. By adjusting the polymerization condition, the degree of polymerization and thus the physicochemical properties of the polymer shell, that is, modification to the core deficiency, and the shell band gap, can be tuned to be suitable for enhancing the fluorescence. The kinetics study of the in situ polymerization on QDs surface was carried out to verify the controllable polymerization. The conducting polymer shells significantly improved the fluorescence intensity, the quantum yield and the biocompatibility of the QDs. This study demonstrated a successful utilization of the coated QDs for luminescence-based cell imaging with a highly amplified signal. We anticipated that the conducting polymer shells can serve as a versatile interfacial medium capable of conjugating biological molecules with QDs. Herein, this kind of conducting polymer materials can be regarded as a series of promising shell materials to improve the optical properties as well as biocompatibility of QDs and such novel QDs are expected to have broad bioapplication prospects.

AUTHOR INFORMATION

Corresponding Authors

*E-mail: lill@nju.edu.cn.

*E-mail: jjzhu@nju.edu.cn.

Notes

The authors declare no competing financial interest.

ACKNOWLEDGMENTS

We gratefully appreciate financial support from National Basic Research Program of China (2011CB933502) and National Natural Science Foundation of China (21335004, 21405078).

REFERENCES

(1) Semonin, O. E.; Luther, J. M.; Choi, S.; et al. Peak External Photocurrent Quantum Efficiency Exceeding 100% via MEG in a Quantum Dot Solar Cell. *Science* **2011**, *334*, 1530−1533.

(2) Saha, S. K.; Bera, A.; Pal, A. J. Improvement in PbS-based Hybrid Bulk-Heterojunction Solar Cells through Band Alignment via Bismuth Doping in the Nanocrystals. *ACS Appl. Mater. Interfaces* **2015**, *7*, 8886−8893.

(3) Kongkanand, A.; Tvrdy, K.; Takechi, K.; et al. Quantum dot solar cells. Tuning Photoresponse through Size and Shape Control of CdSe-TiO_2 Architecture. *J. Am. Chem. Soc.* **2008**, *130*, 4007−4015.

(4) Huang, X. Y.; Han, S. Y.; Huang, W. Enhancing Solar Cell Efficiency: the Search for Luminescent Materials as Spectral Converters. *Chem. Soc. Rev.* **2013**, *42*, 173−201.

(5) Zrazhevskiy, P.; Sena, M.; Gao, X. H. Designing Multifunctional Quantum Dots for Bioimaging, Detection, and Drug Delivery. *Chem. Soc. Rev.* **2010**, *39*, 4326−4354.

(6) Michalet, X.; Pinaud, F. F.; Bentolila, L. A. Quantum Dots for Live Cells, in vivo Imaging, and Diagnostics. *Science* **2005**, *307*, 538−544.

(7) Xu, J. Q.; Tehrani, K. F.; Kner, P. Multicolor 3D Super-resolution Imaging by Quantum Dot Stochastic Optical Reconstruction Microscopy. *ACS Nano* **2015**, *9*, 2917−2925.

(8) Kobayashi, H.; Ogawa, M.; Alford, R.; et al. New Strategies for Fluorescent Probe Design in Medical Diagnostic Imaging. *Chem. Rev.* **2010**, *110*, 2620−2640.

(9) Jang, E.; Jun, S.; Jang, H.; et al. White-Light-Emitting Diodes with Quantum Dot Color Converters for Display Backlights. *Adv. Mater.* **2010**, *22*, 3076−3080.

(10) Shirasaki, Y.; Supran, G. J.; Bawendi, M. G.; et al. Emergence of Colloidal Quantum-Qot Light-Emitting Technologies. *Nat. Photonics* **2013**, *7*, 13−23.

(11) Dai, X. L.; Zhang, Z. X.; Jin, Y. Z.; Niu, Y.; Cao, H. J.; Liang, X. Y.; Chen, L. W.; Wang, J. P.; Peng, X. G. Solution-Processed, High-Performance Light-Emitting Diodes Based on Quantum Dots. *Nature* **2014**, *515*, 96−99.

(12) Yoon, H. C.; Oh, J. H.; Ko, M.; et al. Synthesis and Characterization of Green Zn-Ag-In-S and Red Zn-Cu-In-S Quantum Dots for Ultrahigh Color Quality of Down-Converted White LEDs. *ACS Appl. Mater. Interfaces* **2015**, *7*, 7342−7350.

(13) Freeman, R.; Liu, X. Q.; Willner, I. Chemiluminescent and Chemiluminescence Resonance Energy Transfer (CRET) Detection of DNA, Metal Ions, and Aptamer-Substrate Complexes Using Hemin/G-Quadruplexes and CdSe/ZnS Quantum Dots. *J. Am. Chem. Soc.* **2011**, *133*, 11597−11604.

(14) Hildebrandt, N. Biofunctional Quantum Dots: Controlled Conjugation for Multiplexed Biosensors. *ACS Nano* **2011**, *5*, 5286−5290.

(15) Dong, H. F.; Gao, W. C.; Yan, F.; et al. Fluorescence Resonance Energy Transfer between Quantum Dots and Graphene Oxide for Sensing Biomolecules. *Anal. Chem.* **2010**, *82*, 5511−5517.

(16) Wu, P.; Yan, X. P. Doped Quantum Dots for Chemo/Biosensing and Bioimaging. *Chem. Soc. Rev.* **2013**, *42*, 5489−5521.

(17) Reiss, P.; Protiere, M.; Li, L. Core/Shell Semiconductor Nanocrystals. *Small* **2009**, *5*, 154−168.

(18) Vempati, S.; Ertas, Y.; Uyar, T. Sensitive Surface States and their Passivation Mechanism in CdS Quantum Dots. *J. Phys. Chem. C* **2013**, *117*, 21609−21618.

(19) Sarma, D. D.; Nag, A.; Santra, P. K.; et al. Origin of the Enhanced Photoluminescence from Semiconductor CdSeS Nanocrystals. *J. Phys. Chem. Lett.* **2010**, *1*, 2149−2153.

(20) Bera, D.; Qian, L.; Tseng, T. K.; et al. Quantum Dots and Their Multimodal Applications: A Review. *Materials* **2010**, *3*, 2260−2345.

(21) Chuang, P. H.; Lin, C. C.; Liu, R. S. Emission-Tunable CuInS2/ZnS Quantum Dots: Structure, Optical Properties, and Application in White Light-Emitting Diodes with High Color Rendering Index. *ACS Appl. Mater. Interfaces* **2014**, *6*, 15379−15387.

(22) Focsan, M.; Gabudean, A. M.; Vulpoi, A.; et al. Controlling the Luminescence of Carboxyl-Functionalized CdSe/ZnS Core-Shell Quantum Dots in Solution by Binding with Gold Nanorods. *J. Phys. Chem. C* **2014**, *118*, 25190−25199.

(23) Chen, O.; Zhao, J.; Chauhan, V. P.; et al. Compact High-Quality CdSe-CdS Core-Shell Nanocrystals with Narrow Emission Linewidths and Suppressed Blinking. *Nat. Mater.* **2013**, *12*, 445−451.

(24) Di Stasio, F.; Grim, J. Q.; Lesnyak, V.; et al. Single-Mode Lasing from Colloidal Water-Soluble CdSe/CdS Quantum Dot-in-Rods. *Small* **2015**, *11*, 1328−1334.

(25) Jing, L. H.; Yang, C. H.; Qiao, R. R.; et al. Highly Fluorescent CdTe@SiO_2 Particles Prepared via Reverse Microemulsion Method. *Chem. Mater.* **2010**, *22*, 420−427.

(26) Yu, X. F.; Chen, L. D.; Li, M.; et al. Efficient Fluorescence of NdF3/SiO_2 Core/Shell Nanoparticles and the Applications for in vivo NIR Detection. *Adv. Mater.* **2008**, *20*, 4118.

(27) Dubertret, B.; Skourides, P.; Norris, D. J. In vivo Imaging of Quantum Dots Encapsulated in Phospholipid Micelles. *Science* **2002**, *298*, 1759−1762.

(28) Carion, O.; Mahler, B.; Pons, T.; et al. Synthesis, Encapsulation, Purification and Coupling of Single Quantum Dots in Phospholipid Micelles for their Use in Cellular and in vivo Imaging. *Nat. Protoc.* **2007**, *2*, 2383−2390.

(29) Dixit, S. K.; Goicochea, N. L.; Daniel, M. C.; et al. Quantum Dot Encapsulation in Viral Capsids. *Nano Lett.* **2006**, *6*, 1993−1999.

(30) Xing, Y.; Chaudry, Q.; Shen, C.; et al. Bioconjugated Quantum Dots for Multiplexed and Quantitative Immunohistochemistry. *Nat. Protoc.* **2007**, *2*, 1152−1165.

DOI: 10.1021/acsami.5b04766
ACS Appl. Mater. Interfaces 2015, 7, 19126−19133

(31) Jang, J.; Kim, S.; Lee, K. J. Fabrication of CdS/PMMA Core/Shell Nanoparticles by Dispersion Mediated Interfacial Polymerization. *Chem. Commun.* **2007**, *26*, 2689−2691.
(32) Pang, L.; Shen, Y. M.; Tetz, K.; Fainman, Y. PMMA Quantum Dots Composites Fabricated via Use of Pre-polymerization. *Opt. Express* **2005**, *13*, 44−49.
(33) Higuchi, Y.; Wu, C.; Chang, K. L.; et al. Polyamidoamine Dendrimer-Conjugated Quantum Dots for Efficient Labeling of Primary Cultured Mesenchymal Stem Cells. *Biomaterials* **2011**, *32*, 6676−6682.
(34) Wisher, A. C.; Bronstein, I.; Chechik, V. Thiolated PAMAM Dendrimer-Coated CdSe/ZnSe Nanoparticles as Protein Transfection Agents. *Chem. Commun.* **2006**, *15*, 1637−1639.
(35) Akin, M.; Bongartz, R.; Walter, J. G.; et al. PAMAM-Functionalized Water Soluble Quantum Dots for Cancer Cell targeting. *J. Mater. Chem.* **2012**, *22*, 11529−11536.
(36) Shi, Y. F.; Wang, J. J.; Li, S. J.; Wang, Z. Y.; Zang, X. X.; Zu, X. M.; Zhang, X. Y.; Guo, F. Photoluminescence-Enhanced CdTe Quantum Dots by Hyperbranched Poly(amidoamine)s Functionalization. *J. Mater. Res.* **2013**, *28*, 1940.
(37) Shi, Y. F.; Liu, L.; Pang, H.; Zhou, H. L.; Zhang, G. Q.; Ou, Y. Y.; Zhang, X. Y.; Du, J. M.; Xiao, W. C. Facile Preparation of Highly Luminescent CdTe Quantum Dots within Hyperbranched Poly-(amidoamine)s and their Application in Bio-imaging. *Nanoscale Res. Lett.* **2014**, *9*, 115.
(38) Gangopadhyay, R.; De, A. Conducting Polymer Nanocomposites: A Brief Overview. *Chem. Mater.* **2000**, *12*, 608−622.
(39) Wu, G.; More, K. L.; Johnston, C. M.; et al. High-Performance Electrocatalysts for Oxygen Reduction Derived from Polyaniline, Iron, and Cobalt. *Science* **2011**, *332*, 443−447.
(40) Li, C.; Bai, H.; Shi, G. Q. Conducting Polymer Nanomaterials: Electrosynthesis and Applications. *Chem. Soc. Rev.* **2009**, *38*, 2397−2409.
(41) Miao, Y.-E.; Fan, W.; Chen, D.; et al. High-Performance Supercapacitors Based on Hollow Polyaniline Nanofibers by Electrospinning. *ACS Appl. Mater. Interfaces* **2013**, *5*, 4423−4428.
(42) Li, L. L.; Chen, Y.; Lu, Q.; Zhu, J. J.; et al. Electrochemiluminescence Energy Transfer-Promoted Ultrasensitive Immunoassay Using Near-Infrared-Emitting CdSeTe/CdS/ZnS Quantum Dots and Gold Nanorods. *Sci. Rep.* **2013**, *3*, 1529.
(43) Liang, G. X.; Li, L. L.; Liu, H. Y.; Zhu, J. J.; et al. Fabrication of Near-Infrared-Emitting CdSeTe/ZnS Core/Shell Quantum Dots and Their Electrogenerated Chemiluminescence. *Chem. Commun.* **2010**, *46*, 2974−2976.
(44) Liang, G. X.; Liu, H. Y.; Zhang, J. R.; Zhu, J. J. Ultrasensitive Cu^{2+} Sensing by Near-Infrared-Emitting CdSeTe Alloyed Quantum Dots. *Talanta* **2010**, *80*, 2172−2176.
(45) Sun, D.; Ban, R.; Zhang, P. H.; et al. Hair Fiber as a Precursor for Synthesizing of sulfur- and Nitrogen-Co-doped Carbon Dots with Tunable Luminescence Properties. *Carbon* **2013**, *64*, 424−434.
(46) Vempati, S.; Ertas, Y.; Uyar, T. Sensitive Surface States and their Passivation Mechanism in CdS Quantum Dots. *J. Phys. Chem. C* **2013**, *117*, 21609−21618.
(47) Deng, S. Y.; Ju, H. X. Electrogenerated Chemiluminescence of Nanomaterials for Bioanalysis. *Analyst* **2013**, *138*, 43−61.
(48) Dohnalova, K.; Poddubny, A. N.; et al. Surface Brightens up Si Quantum Dots: Direct Bandgap-Like Size-Tunable Emission. *Light: Sci. Appl.* **2013**, *2*, e47.
(49) Hu, X. W.; Mao, C. J.; Song, J. M.; Niu, H. L.; Zhang, S. Y.; Huang, H. P. Fabrication of GO/PANi/CdSe Nanocomposites for Sensitive Electrochemiluminescence Biosensor. *Biosens. Bioelectron.* **2013**, *41*, 372−378.
(50) Haldorai, Y.; Nguyen, V. H.; Shim, J.-J. Synthesis of Polyaniline/Q-CdSe Composite via Ultrasonically Assisted Dynamic Inverse Emulsion Polymerization. *Colloid Polym. Sci.* **2011**, *289*, 849−854.
(51) Furukawa, Y.; Ueda, F.; Hyodo, Y.; Harada, I.; Nakajima, T.; Kawagoe, T. Vibrational-Spectra and Structure of Polyaniline. *Macromolecules* **1988**, *21*, 1297−1305.
(52) Atkins, P.; Paula, J. *Physical Chemistry [M]*; Oxford University Press: Oxford, U.K., 2010; p 799.
(53) Bruice, P. Y. *Organic Chemistry [M]*; Pearson Education: London, 2014; p 932.
(54) Mo, Z. H.; Qiu, W.; Yang, X. C.; et al. Morphological Characterization and Kinetics Study of Polyaniline Film Formation by Emulsion Polymerization. *J. Polym. Res.* **2009**, *16*, 39−43.
(55) Mu, S. L.; Chen, C. X.; Wang, J. M. The Kinetic Behavior for the Electrochemical Polymerization of Aniline in Aqueous Solution. *Synth. Met.* **1997**, *88*, 249−254.

DOI: 10.1021/acsami.5b04766
ACS Appl. Mater. Interfaces 2015, 7, 19126−19133